Following the infection process of vibriosis in Manila clam (*Ruditapes philippinarum*) larvae through GFP–tagged pathogenic *Vibrio* species.

Javier Dubert[a,*], David R. Nelson[b], Edward J. Spinard[b], Linda Kessner[b], Marta Gomez–Chiarri[c], Fiz da Costa[d], Susana Prado[a] and Juan L. Barja[a].

[a]Departamento de Microbiología y Parasitología. CIBUS–Facultad de Biología y Instituto de Acuicultura. Universidad de Santiago de Compostela. Santiago de Compostela, 15782. Spain.

[b]Department of Cell and Molecular Biology and [c]Department of Fisheries, Animal and Veterinary Sciences. University of Rhode Island. Kingston, Rhode Island, 02881. United States.

[d]Novostrea Bretagne, Route du Vieux Passage, Banastère, 56370 Sarzeau, France.

Accepted in: Journal of Invertebrate Pathology.

Revised Ms. JIP–15–236 R2

DOI: 10.1016/J.JIP.2015.11.008

*Corresponding author at: Departamento de Microbiología y Parasitología. CIBUS–Facultad de Biología y Instituto de Acuicultura. Universidad de Santiago de Compostela. Santiago de Compostela, 15782. Spain. Tel: (+34) 881816911; Fax: (+34) 981 528085.

E−mail: javier.dubert@usc.es (J. Dubert)

Abstract

Vibriosis represents the main bottleneck for the larval production process in shellfish aquaculture. While the signs of this disease in bivalve larvae are well known, the infection process by pathogenic *Vibrio* spp. during episodes of vibriosis has not been elucidated. To investigate the infection process in bivalves, the pathogens of larvae as *V. tubiashii* subsp. *europaensis*, *V. neptunius* and *V. bivalvicida* were tagged with green fluorescent protein (GFP). Larvae of Manila clam (*Ruditapes philippinarum*) were inoculated with the GFP−labeled pathogens in different infection assays and monitored by microscopy. Manila clam larvae infected by distinct GFP−tagged *Vibrio* spp. in different challenges showed the same progression in the infection process, defining three infection stages. GFP−tagged *Vibrio* spp. were filtered by the larvae through the vellum and entered in the digestive system through the esophagus and stomach and colonized the digestive gland and particularly the intestine, where they proliferated during the first 2 hours of contact (Stage I), suggesting a chemotactic response. Then, GFP–tagged *Vibrio* spp. expanded rapidly to the surrounding organs in the body cavity from the dorsal to ventral region (Stage II; 6–8 h), colonizing the larvae completely at the peak of infection (Stage III) (14–24 h). Results demonstrated for the first time that the vibriosis is asymptomatic in Manila clam larvae during the early infection stages. Thus, the early colonization and the rapid proliferation of *Vibrio* pathogens within the body cavity supported the sudden and fatal effect of the vibriosis, since the larvae exhibited the first signs of disease when the infection process is advanced. As a first step in the elucidation of the potential mechanisms of bacterial pathogenesis in bivalve larvae the enzymatic activities of the extracellular products released from the wild type *V. neptunius*, *V. tubiashii* subsp. *europaensis* and *V. bivalvicida* were determined and

51 their cytotoxicity was demonstrated in fish and homeothermic cell lines for the first
52 time. That activity was lost after heat treatment.
53 **Keywords:** Vibriosis; Manila clam; larvae; *Vibrio* spp.; green fluorescent protein
54 (GFP).
55

56 **1. Introduction**

57

58 Vibriosis is the most important bacterial disease affecting the larval stages of
59 different species of marine mollusks in shellfish aquaculture. Outbreaks of disease due
60 to pathogenic *Vibrio* spp. have been described worldwide in larvae of several bivalve
61 species cultured in hatcheries (Prado et al., 2005; Beaz–Hidalgo et al., 2010; Travers et
62 al., 2014; Prado et al., 2015; Rojas et al., 2015).
63 Bivalve larvae are more susceptible to vibriosis than adults since the resistance to
64 bacterial infection significantly increases with age of the bivalves (Gómez–León et al.,
65 2008). The pathogens *V. tubiashii* subsp. *europaensis, V. neptunius* and *V. bivalvicida*
66 have been identified as the etiological agents responsible for larval and spat mortality
67 episodes in clam and oyster cultures leading to important economic losses for the
68 shellfish hatcheries (Prado et al., 2005; Prado et al., 2015; Dubert et al., in press).
69 Extracellular products (ECPs) should be studied since virulence is usually associated
70 with these products released by some pathogenic *Vibrio* species (Shinoda and Miyoshi,
71 2011). Signs of disease include an important reduction of larval motility, erratic
72 swimming, closing of the valves, velum detachment, and bacterial swarming inside and
73 around the larvae (Prado et al., 2005; Beaz–Hidalgo et al., 2010; Rojas et al., 2015).
74 While the clinical signs of vibriosis are well known, the processes of colonization and
75 infection by pathogenic *Vibrio* spp. in bivalve larvae have not been elucidated. Vibriosis

has only been monitored by means of molecular tagging of the pathogens in adult mollusks (Cabello et al., 2005; Travers et al., 2008; Cardinaud et al., 2014).

In order to investigate the pathogenesis of vibriosis in bivalve larvae, we investigated the colonization and infection process by the pathogens *V. neptunius*, *V. tubiashii* subsp. *europaensis* and *V. bivalvicida*, tagged with green fluorescent protein (GFP), in bivalve larvae. Considering the economic importance of clam production for shellfish aquaculture and the high susceptibility of larval batches to vibriosis, Manila clam (*Ruditapes philippinarum*) larvae were chosen as infection model. Additionally, enzymatic activities of wild type pathogenic *Vibrio* spp. and their ECPs were determined. Finally, the cytotoxicity of the ECPs was evaluated in fish and homoeothermic cell lines.

2. Materials and methods

2.1. Bacterial strains, plasmid and culture conditions

Larval pathogens *V. neptunius* PP–145.98, *V. tubiashii* subsp. *europaensis* CECT 8136^{T} and *V. bivalvicida* CECT 8855^{T} were grown at 25ºC and shaken 200 rpm in YP broth, constituted by yeast extract (0.5%, w/v) (Thermo Fisher Scientific, USA) and peptone (0.1%, w/v) (BD, France) at pH 7.6, supplemented with 3% (w/v) of sea salts (YP30) (Instant Ocean, USA). Streptomycin (Sm^{200}; 200 µg ml^{-1}, Sigma–Aldrich, USA) was only added to YP30 for mating assays since wild type strains were resistant to Sm.

In a previous study, Zhao et al. (unpublished results) designed the plasmid pRhokHi–2–GFP, which has chloramphenicol (Cm^{R}) and kanamycin (Km^{R}) resistance markers, and derivative from pRhokHi–2–FbFP (Piekarski et al., 2009) with *gfp* gene under the

control of the constitutive promoter of the aminoglycoside phosphotransferase II (P*aphII*). Plasmid pRhokHi–2–FbFP is 7.38 kb, carrying Cm^R and Km^R resistances, P_{T7} *FbFP* constructed under the control of P*aphII* from the conjugally transferable and stably maintained plasmid pBBR1MCS. The resulting plasmid pRhokHi–2–GFP was introduced in *Escherichia coli* Sm10 (*thi thr leu tonA lacY supE recA* RP4–2 Tc::Mu::KmR, λ pir) by electroporation. In the present study, *E. coli* Sm10 pRhokHi–2–GFP was cultured in Luria–Bertani plus 10% NaCl (LB10) supplemented with Cm^{20} (20 μg ml^{-1}; Sigma, USA) at 37ºC while shaking at 200 rpm.

In all cases, 1.5% agar (w/v) (BD, France) was added when the solid media were required.

2.2. Mating assays and selection of GFP–tagged strains

Plasmid pRhokHi–2–GFP carried was introduced into larval pathogens from *E. coli* Sm10 by conjugation following the procedure described by Milton et al. (1992) with slight modifications. Briefly, overnight cultures of each *Vibrio* spp. and *E. coli* Sm10 pRhokHi–2–GFP were grown for the different mating assays as described above. Then, *Vibrio* culture was mixed at 1:1 ratio in Nine Salt Solution (NSS) (Varina et al., 2008) and *E. coli* in 10 mM $MgSO_4$ and 100 μl of each one were diluted again in 2.5 ml of NSS and $MgSO_4$ respectively. Bacterial suspensions were combined and vacuum filtered onto a 0.22 μm nitrocellulose membrane (Millipore, USA), which was placed onto YP plates plus 1.5% (w/v) of sea salts (YP15) and incubated overnight at 25°C. Subsequently, the cells were removed from the filter by vigorous mixing in YP30 broth and 100 μl were spread onto three YP30 plates supplemented with Sm^{200} and Cm^5 and incubated at 25ºC until *Vibrio* transconjugants were observed (usually 24 to 72 h).

126

127 *2.3. Confirmation of the transconjugants*

128

129 Transconjugants were isolated from the mating assays and their morphology,
130 motility and green fluorescence was checked by epifluorescence microscopy (40x)
131 (Zeiss Axioskop 2, Germany) using the filter for green signal (FITC, 488 nm). Growth
132 on TCBS plates (Oxoid, USA) was also evaluated. DNA of the GFP–tagged *Vibrio* spp.
133 was extracted with Instagene kit (Bio–Rad, UK) and their 16S rRNA gene was
134 amplified and sequenced to confirm their identities using specific bacterial primers (27F
135 and 1510R) (Lane, 1991). Sequences were analyzed with the Lasergene Seqman
136 (DNAstar, USA) and identified using the BLAST database (Altschul et al. 1997).
137 Moreover, growth curves of wild type *Vibrio* spp. and GFP–tagged strains were
138 determined by optical density measurements at 600 nm (OD_{600}) to detect differences in
139 the growth speed. Hence, stationary phase cultures were adjusted to 1.0 absorbance,
140 diluted 1:100 in YP30 broth and incubated at 25ºC and 200 rpm. Bacterial
141 concentrations (OD_{600}) were estimated per duplicate at 2, 4, 6, 8, 10, 24 and 48 h. At the
142 same time, the green fluorescence of the GFP–tagged strains were evaluated at 96 h by
143 epifluorescence microscopy (40x) to guarantee that the expression of the green
144 fluorescence protein gene lasted for this length of time in absence of selective pressure
145 due to the antibiotic.

146

147 *2.4. Colonization and infection assays*

148

149 A previously developed challenge model (Prado et al., 2015) was used to determine
150 the colonization and infection process for each of the GFP–tagged *Vibrio* species.

Healthy ten–day–old *R. philippinarum* veliger larvae (120 µm, umbonate veliger) were placed in wells in 12 well microplates (NUNC; ThermoFisher Scientific, USA) filled with 3 ml of sterile seawater (SSW) at a density of 15–20 larvae ml^{-1}. Wild type pathogenic *Vibrio* spp., used as positive controls, were grown overnight in YP30 plates as described above, whereas GFP–tagged strains were cultured in YP30 plates supplemented with Sm^{200} and Cm^{5} under the same incubation conditions. Strains, including wild type and GFP–tagged, were re–suspended in SSW and inoculated in different duplicate wells at a final concentration of 10^{6} CFU ml^{-1}. Bacterial concentrations were confirmed by serial dilution and spread plating onto YP30 agar plates. In addition, wells containing only larvae in SSW were used as negative controls. Larval cultures were kept in dark at 20ºC in a rotary shaker at 50 rpm. Positive and negative controls were checked at 0, 24 and 48 h. Wells inoculated with each GFP–tagged *Vibrio* spp. were sampled at 0, 2, 6, 8, 14, 24 and 36, 48 h for monitoring the infection. Advance of the clinical signs of vibriosis and the integrity of the larvae were checked directly from the microplates by phase contrast (10/20x) in an inverted microscopy (Olympus CK40, Japan). Larvae from each corresponding well were collected from the wells, centrifuged at 3000 rpm 10 s and observed by epifluorescence microscopy (40x) (Zeiss Axioskop 2, Germany) in a concave slide. Samples were evaluated with different filter sets FITC (488 nm), Cy3 (546 nm) and Cy5 (633 nm) to distinguish between the fluorescence due to the GFP and the autofluorescence of the larvae.

2.5. *Cytotoxicity of the extracellular products (ECPs*)

The ECPs were obtained from liquid media as described Romalde (1992). Briefly, wild type *Vibrio* spp. were grown in flasks (50 ml) containing 10 ml of YP30 broth and incubated at 25ºC (24 h, 200 rpm). Cultures were centrifuged at 8000 rpm (5510x *g*) for 5 min (Eppendorf Centrifuge 5418), filtered through a 0.20 µm cellulose acetate filter (Sartorius, Germany) and frozen at −20ºC. The protein concentration was determined using the Protein Assay (Bio–Rad, USA), based on the Bradford dye−binding method, with bovine serum albumin (BSA) as the standard. Aliquots of ECP were also heat–treated (100°C for 10 min) and all ECPs preparations were assayed for cytotoxicity as previously described Magariños et al. (1992) using fish and homoeothermic cell lines: EPC (epithelioma papulosum cyprini) and Vero (African green monkey). Monolayers grown in 24 well microplates (NUNC; Thermo Fisher Scientific, USA) and they were inoculated with each ECPs at final dilution 1:10 and incubated at 25ºC (fish cell lines) or 37ºC (homeothermic cell lines). Cytotoxicity assays were carried out in duplicate and YP30 broth was used as negative control. A cytotoxic effect, i.e. degenerative changes or cell detachment, was determined to be positive based in the total or partial destruction of monolayers by direct observation of the cell lines by phase contrast inverted microscope (10/20x) at 24 h.

Additionally, enzymatic activities of *Vibrio* strains using the whole cells from YP30 plates, as well as non–treated ECPs or heat–treated ECPs (100°C for 10 min), were also evaluated by API ZYM (bioMérieux, France) following the manufacturer instructions and incubated 24 h at 25ºC.

3. Results

3.1. Verification of the GFP–tagged Vibrio species.

Transconjugants were motile green fluorescent rods when observed by epifluorescence microscopy. They grew as yellow colonies on TCBS plates with the same appearance as their parental strains. When the wild type parental strains and their corresponding GFP−tagged derivative strains of the three vibrio species were grown in YP30, no differences in growth rate or final cell density were observed (Supplementary Fig. 1). On the basis of the 16S rDNA sequences, GFP–tagged transconjugants showed 99% similarity with their corresponding wild type *Vibrio* species: *V. neptunius* PP–145.98 (AJ296157), *V. tubiashii* subsp. *europaensis* CECT 8136^{T} (AY792622) and *V. bivalvicida* CECT 8855^{T} (HF568951). The green fluorescent protein gene of the GFP–tagged *Vibrio* spp. was expressed in absence of antibiotic for at least 96 h (data not shown).

3.2. Progression of the infection by Vibrio spp. in bivalve larvae

Vibrio−challenged *R. philippinarum* larvae were observed by inverted and epifluorescence microscopy to follow the progression of the infection process by visualization of the GFP–tagged *Vibrio* spp. and examination of clinical signs.

The observed infections of the Manila clam larvae by all three GFP−tagged *Vibrio* species (*V. neptunius* PP–145.98, *V. tubiashii* subsp. *europaensis* CECT 8136^{T} and *V. bivalvicida* CECT 8855^{T}) showed the same progression, allowing us to define three stages in the infection process common to all 3 pathogenic species (Fig. 1). GFP−tagged *Vibrio* spp. were filtered by the larvae through the vellum and entered in the digestive system through the esophagus and the stomach colonizing the digestive gland and particularly the intestine. They accumulated and proliferated rapidly in these

organs during the first 2 h of infection (Fig. 1A and 1B). Within 6–8 h (Fig. 1C and 1D, respectively), GFP–tagged *Vibrio* spp. extended and proliferated to the surrounding organs in the body cavity, which is constituted by the visceral and mantle cavities, from the dorsal (umbo; digestive gland and intestine) to the ventral region regardless of the vibrio pathogenic species analyzed (Stage II). Interestingly, the early proliferation of *Vibrio* pathogens (Fig. 1A–C) was observed before the larvae exhibited the first signs of disease. Indeed, most Manila clam larvae showed normal appearance and remained active with a regular swimming pattern during early Stage II (6 h) (Fig. 1C). However, first signs of disease, as reduction of the larval motility accompanied by circular/erratic swimming, were detected by inverted microscopy at 8 h, when the *Vibrio* proliferation was advanced (late Stage II, 8 h) (Fig. 1D). After 14 h of infection, GFP fluorescence in the ventral region was stronger and the body cavity of some larvae was completely colonized by GFP–tagged *Vibrio* spp. (Fig. 1E) (Stage III). Infections were not synchronous within larvae in the same well and individual larvae showed different infection stages within the same challenge. Some larvae were in Stage I, others had progressed to II or III at 14 h. However, sedentary larvae were in Stage III at 14 h and their valves were kept closed although showed internal movement, indicating that they were still alive. Stage III infections peaked by 24 h when GFP–tagged *Vibrio* spp. had colonized completely the body cavity of most larvae showing strong green fluorescence (Fig. 1F). At this time mortalities due to the three GFP–tagged *Vibrio* species were common in all challenges, namely in percentages of 80.0±1.7 for GFP–*V. neptunius* PP–145.98, 81.8±1.9 for GFP–*V. tubiashii* subsp. *europaensis* CECT 8136^{T} and 79.6±2.3 GFP–*V. bivalvicida* CECT 8855^{T}. Moreover, ubiquitous bacterial swarming was observed inside and around dead and moribund larvae (Fig. 1G) and velum detachment (Fig. 1H) after all other soft tissues have been destroyed and GFP–tagged *Vibrio* spp.

were not detected in these larvae in high state of decomposition. Hence, no attachment to the shell was observed by epifluorescence microscopy (Fig. 1H) despite of GFP–tagged *Vibrio* spp. were isolated from these wells. Total mortality (100%) was detected after 36 h of infection in all GFP−challenges.

The same dynamic of infection, as determined by clinical signs through the light microscopy, were observed in the positive controls inoculated with the wild type pathogenic *Vibrio* species. Indeed, mortalities (%) were similar for the wild type strains at 24 h, namely the 79.3±1.2 for *V. neptunius* PP–145.98, 82.4±1.6 for *V. tubiashii* subsp. *europaensis* CECT 8136^{T} and 80.6±2.4 *V. bivalvicida* CECT 8855^{T}. As expected, 100% mortality was detected at 48 h in all positive controls, since positive and negative controls were only checked at 0, 24 and 48 h and not at 36 h. Larvae in the negative controls showed healthy appearance with regular and fast swimming after 48 h with mortalities (%) of 3.9±0.9. In infected challenges, the pathogens were recovered from affected larvae, confirming that these mortalities were caused by the isolate used in the challenge experiments.

3.3. Biological activities of the ECPs in vitro

In all cases, ECPs were cytotoxic for fish (EPC) and homoeothermic (Vero) cell lines after 24 h regardless of the *Vibrio* species. Cytotoxic effects were similar in both cell lines independently of the *Vibrio* spp., producing degenerative changes manifested by clustering and round cells, shrinking and finally cell detachment (Supplementary Fig. 2). Destruction of monolayers was not observed when the ECPs were heat treated, suggesting that the cytotoxic activity may be due to enzymatic activities.

Enzymatic activities of the ECPs were analyzed by using the API ZYM system and the results were compared with the activities showed by the whole cells. Enzymatic activities were found similar among ECPs from the pathogenic strains. Hence, all ECPs showed the esterase, esterase lipase, lipase, leucine arylamidase, valine arylamidase, cysteine arylamidase, trypsin and α−chymotrypsin activities (Table 1). Alkaline phosphatase was only detected for ECPs obtained from *V. tubiashii* subsp. *europaensis* CECT 8136^{T} and *V. neptunius* PP−145.98. Only esterase lipase, lipase, and leucine arylamidase activities produced by the pathogenic *Vibrio* spp. were also present in the ECPs.

Some differences between the enzymatic activities of ECPs and whole cells were found (Table 1). Indeed, the ECPs of *V. tubiashii* subsp. *europaensis* CECT 8136^{T} and *V. bivalvicida* CECT 8855^{T} showed higher variety of enzymatic activities than the whole cells, with instances in which activity was detected in ECPs but not in live cells: esterase (C4), valine arylamidase, trypsin and α−chymotrypsin. However, N−acetyl−β−glucosaminidase was detected in whole cells of *V. tubiashii* subsp. *europaensis* CECT 8136^{T} and alkaline phosphatase in *V. bivalvicida* CECT 8855^{T} but not in their respective ECPs. The whole cells of *V. neptunius* PP−145.98 showed higher enzymatic activities than the ECPs, including, acid phosphatase, naphtol−AS−BI−phosphohydrolase and N−acetyl−β− glucosaminidase.

4. Discussion

Green fluorescent protein is widely used in biochemistry, cellular biology or microbiology since it allows the direct observation of molecular processes in live systems (Chudakov et al., 2010). Several authors have reported the undesirable effect of

this protein on physiology of some *Vibrio* spp. by means of changes in the bacterial growth or virulence (Aboubaker et al., 2012; Rekeki et al., 2012). Indeed, Allison and Sattenstall (2007) proposed that the wild type and the GFP−tagged strains should be checked previously since the GFP tagging may affect the quality and accuracy of data generated depending on the application for which is used. Our results demonstrated that the GFP expression did not have any apparent effect on the physiological characteristics of the pathogenic *Vibrio* spp. assayed.

Different routes of colonization have been suggested for different species of bivalve larvae by means of histological studies. Tubiash et al. (1965) suggested that infection by *V. tubiashii* in larvae of *Mercenaria mercenaria*, *Ostrea edulis*, *Aequipecten irradians* and *Teredo navalis* occurs through the gastrointestinal tract. Other routes of infection, designated types I, II and III pathogenesis, have been described by Elston and Leibovitz (1980) during experimental vibriosis in *Crassostrea virginica* larvae. In that study, all larval stages were affected by Type I pathogenesis, in which the bacteria attached to the shell of sedentary larvae, grew along the internal shell surface with progressive disruption of mantle tissue from the periphery inward and invaded and proliferated within the visceral cavity, in which destroyed all tissues; or Type II pathogenesis, described for early veliger larvae, in which larvae remain active despite showing a severe velar deformation with abnormal swimming patterns without bacterial invasion of the tissues until late in the disease process and subsequent necrosis of digestive organs and a proliferation of the bacteria within the visceral cavity. In Type III pathogenesis, sedentary late veliger larvae exhibited progressive and extensive body atrophy before the invasion of bacteria by focal lesions into the organs of the digestive gland. However, none of these studies used specifically tagged pathogenic *Vibrio* spp. making it difficult to distinguish the pathogen from the larval microbiota.

The use of a fluorescent tagging to specifically mark bacteria for pathological studies allows selective observation of bacteria inside the larvae and ensures that the inoculated bacteria are those observed. Recently, Rojas et al. (2015) observed that the pathogen *V. splendidus*, stained with 5–([4,6–dichlorotriazin–2–yl]amino)fluorescein hydrochloride (5–DTAF), reached the digestive gland of *Argopecten purpuratus* 10–day old larvae after 30 min and then were concentrated in the digestive gland. Our results confirmed this observation, including also the intestine, in a different bivalve species using several GFP−tagged pathogenic *Vibrio* species. Further, we described for the first time in bivalve larvae the complete colonization process by pathogenic *Vibrio* by means of GFP−tagged cells. The colonization of the digestive gland and particularly the intestine (Stage I) by GFP−tagged pathogenic *Vibrio* spp. appears to result from the bacterial cells able to enter and attach to the digestive tract of bivalve larvae through filter feeding. The digestive system of bivalve larvae is constituted by the mouth, esophagus, stomach, style sac, digestive gland, intestine and anus (Elston, 1980a). Larval vellum may capture bacteria with ciliary bands and transport them to the mouth of the larvae. According to Kasyanov et al. (1998), capture of food, including bacteria, and its transfer to the oral opening in bivalve larvae is accomplished by means of the ciliary bands of the velum. The coordination of the beating cilia of the pre– and post–oral ciliary bands ensures the concentration of food particles from the water by the ciliary bands, and leads the food, including bacteria, from the oral opening to the esophagus. Then, the ingested bacteria reach the stomach, and subsequently colonize the digestive gland and particularly the intestine, where pathogenic GFP−tagged *Vibrio* spp. proliferate rapidly (Stage I). In the Stage II, pathogenic *Vibrio* spp. expanded quickly to the surrounding organs from the dorsal to ventral region in the body cavity, including the visceral and mantle cavities. At the peak of infection (Stage III), pathogenic *Vibrio*

spp. colonized completely the larvae. The larvae of bivalves lack a circulatory system and the transport of substances from one organ to the other and particularly that of nutrients from the digestive system to other parts of the body occurs through the extensive body cavity (Kasyanov et al., 1998), which includes the visceral and mantle cavities. This cavity is large and easily observed in the avascular larval bivalve, but not in the adult, which has a well–developed open circulatory system (Elston, 1980b; Kasyanov et al., 1998). Transport of various substances could be accomplished by means of the flexion and extension of velum muscles. Moreover, the body cavity contains coelomocytes with smooth endoplasmic reticulum (SER cells) that participate in the process and transport the soluble nutrients secreted by the cells of the digestive system (Elston 1980b; Kasyanov et al., 1998). Elston (1980a) defined the visceral cavity as an enclosed fluid filled chamber containing the digestive organs, musculature and free cells, which is limited laterally and dorsally by the mantle and ventrally by the velum. The mantle is a paired organ, each part consisting of a thin sheet of tissue adjacent to the medial aspect of its corresponding valve (Elston, 1980a), which delimits in the larvae the mantle cavity.

Our results did not clarify the mechanisms by which pathogenic *Vibrio* spp. spread from the digestive gland and intestine to other tissues in the larvae. We hypothesize that *Vibrio* spp. may exploit the mechanisms used for the transport of nutrients by coelomocytes to infect the larvae or may be able to pass through intestine tissues by active translocation or to infect by breaching the intestinal epithelium, as seen in other species (Elston, 1980b; Grisez et al., 1996; Olsson et al., 1996; Kasyanov et al., 1998; O'Toole et al., 1999; Torrecilla et al., 2011; Lindell et al., 2012). Moreover, we cannot discard that pathogenic *Vibrio* spp. goes from the stomach to digestive gland, intestine and anus. In fact, Elston and Leibovitz (1980) observed erosion of the intestine

374 epithelium in Type II pathogenesis during experimental vibriosis in *Crassostrea*
375 *virginica* larvae. Further studies should be done to elucidate these hyphothesis.
376 Our findings suggest that these pathogenic *Vibrio* spp. may exhibit a chemotactic
377 response for one or more components of the digestive system, namely digestive gland
378 and particularly the intestine, during the first stage of the vibriosis. The chemotactic
379 response of *V. anguillarum* toward intestinal mucus fish or *V. fischeri* in squid was also
380 reported (O'Toole et al., 1999; DeLoney–Marino et al., 2003; Larsen et al., 2004).
381 Moreover, different tropisms of *V. harveyi* and *V. parahaemolyticus* tagged with GFP
382 were described for gills of adult mollusks, as *Haliotis tuberculata, H. discus hannai* and
383 *Tiostrea chilensis* (Cabello et al., 2005; Travers et al., 2008; Cardinaud et al., 2014).
384 Signs of disease observed in the challenges coincided with signs of disease
385 described previously for vibriosis (Prado et al., 2005; Beaz–Hidalgo et al., 2010; Rojas
386 et al., 2015). However, we present for the first time evidences that support that the
387 vibriosis is asymptomatic in the bivalve larvae during the early infection stages. Hence,
388 Manila clam larvae did not exhibited the typical signs of vibriosis and showed a normal
389 appearance with regular swimming pattern during the first infection hours (early Stage
390 II, 6 h), despite the *Vibrio* colonization in the digestive gland and their proliferation
391 within the body cavity. Thus, first signs of disease were observed after 8 h, when the
392 *Vibrio* proliferation is advanced (late Stage II, 8 h). The rapid colonization of the *R.*
393 *philippinarum* larvae by the GFP–tagged *Vibrio* spp. should be taken into account
394 before the establishment of preventive treatments against vibriosis since once the
395 pathogen is inside the larvae the infection process cannot be stopped.
396 All ECPs tested contained toxins with lethal effects for fish and homoeothermic
397 cell lines. Recently, the toxicity of ECPs obtained from French *V. tubiashii* strains was
398 demonstrated by injection into the adductor muscle of ten to twelve month–old oyster

399 spat (Travers et al., 2014). Moreover, the absence of cytotoxic and enzymatic activities
400 of ECPs after heat treatment demonstrated that the toxin(s) is (are) thermolabile,
401 suggesting that different enzymes can participate in the cytotoxicity. Therefore, we
402 characterized the enzymatic profile both ECPs and whole cells for our target *Vibrio*
403 spp., identifying some enzymes that may be involved in the virulence of these bivalve
404 pathogens. Gómez−León et al. (2005) demonstrated that ECPs isolated from the bivalve
405 larval pathogens *V. alginolyticus* and *V. splendidus*, which had similar enzymatic
406 activities to our isolates (alkaline phosphatase, esterase, esterase lipase, lipase, leucine
407 arylamidase, valine arylamidase, trypsin and α−chymotrypsin), were involved in the
408 cytotoxic and pathogenic activity of clam hemocytes. Some enzymatic activities as
409 detected by the API−ZYM were observed in the ECPs but not in the whole cells. Since
410 the extraction process itself involves the concentration of extracellular products, these
411 enzymes may also be present in the whole cells but not in sufficient concentration to
412 produce the activity necessary for detection (Balboa, 2012). Interestingly, detection of
413 alkaline phosphatase in ECPs needs further investigation since this enzyme is often
414 located in the periplasmic space in Gram negative bacteria and in *V. cholerae* is
415 involved in the survival during the phosphate starvation (Majumdar et. al., 2005). In
416 contrast, certain enzymatic activities were only detected in the whole cells but not in the
417 ECPs. This could be due to differences in regulation of enzyme secretion due to
418 differences in the incubation media (YP30 for the ECPs and saline solution for whole
419 cells) during the incubation with the API ZYM substrates or the concentration of live
420 cells. Different mechanisms for extracellular secretion of toxins have been reported for
421 *Vibrio* spp., such the type I, II, III or VI secretion systems (T1SS, T2SS, T3SS or T6SS)
422 (Boardman et al., 2007; Zhang et al., 2012; Sheng et al., 2013; Sikora, 2013; Lu et al.,
423 2014; Altindis et al., 2015; Chand et al., 2015; Kudryashev et al., 2015). The T2SS is

424 considered a major survival mechanism for pathogenic and environmental species,
425 including *Vibrio* spp., since substrates secreted via T2SS include virulence factors and
426 degradative enzymes, such as chitinases, proteases, lipases/esterases, phospholipases,
427 and nucleases (Korotkov et al., 2012; Johnson et al., 2014). Moreover,
428 N−acetyl−β−glucosaminidase was detected in whole cells of *V. tubiashii* subsp.
429 *europaensis* and *V. neptunius* but not in their respective ECPs. This fact could be
430 supported due to some/many N−acetyl−ß−glucosaminidases are intracellular enzymes
431 involved in the cell wall recycling or in chitin degradation (Cheng et al., 2000; Suginta
432 et al., 2010). Mechanisms of regulation of extracellular secretion should be determined
433 in further studies to explain differences in enzymatic activities in the whole cells but not
434 in the ECPs. Further studies should be done about the characterization of ECPs since the
435 production of metalloproteases related to the toxicity have been documented in several
436 fish and shellfish pathogenic *Vibrio* spp. as *V. aestuarianus, V. anguillarum, V.*
437 *splendidus* and *V. tubiashii* (Norqvist et al., 1990; Milton et al., 1992; Binesse et al.,
438 2008; Hasegawa et al., 2008; Labreuche et al., 2010; Shinoda and Miyoshi, 2011;
439 Mersni–Achour et al., 2014).
440 In conclusion, this is the first report in which the complete colonization process of
441 the pathogenic *Vibrio* spp. was determined in bivalve larvae using specific molecular
442 tagging such as GFP. Results let to validate the infection model in Manila clam and
443 generalize the dynamic of colonization during the vibriosis for 3 different vibrio
444 pathogens previously isolated from outbreaks of vibriosis in bivalve hatcheries.
445 Moreover, we present for the first time evidences that support that the vibriosis is
446 asymptomatic during the early infection stages since clam larvae did not exhibited signs
447 of disease. Rapid colonization of the larvae by these pathogens must be kept in mind to
448 establish preventive protocols against vibriosis and to guarantee the success of the larval

cultures. Additionally, this report gives the first description in which the cytotoxicity of ECPs released from *V. neptunius*, *V. tubiashii* subsp. *europaensis* and *V. bivalvicida* was demonstrated in fish and homoeothermic cell lines. These results let to advance in the knowledge of the pathogenesis of vibriosis in bivalve larvae.

Conflict of interest

All the authors declare that they have no conflicts of interest.

Acknowledgements

Study was supported by grant AGL2014−59655 from the Ministry of Economy and Competitiveness of Spain and GRC−2014/007 from Xunta de Galicia. This research is also based in part on work conducted using the Rhode Island Genomics and Sequencing Center and Molecular Characterization Facility, which are supported in part by the National Science Foundation under EPSCoR grant numbers 0554548 and EPS−1004057.

References

Aboubaker, M.H., Sabrié, J., Huet, M., 2013. Establishment of stable GFP–tagged *Vibrio aestuarianus* strains for the analysis of bacterial infection–dynamics in the Pacific oyster, *Crassostrea gigas*. Vet. Microbiol. 164, 392–398.

Allison, D.G., Sattenstall, M.A., 2007. The influence of green fluorescent protein incorporation on bacterial physiology: a note of caution. J. Appl. Microbiol. 103, 318–324.

Altindis, E., Dong, T., Catalano, C., 2015. Secretome analysis of *Vibrio cholerae* type VI secretion system reveals a new effector–immunity pair. MBio 6, 1–10.

Altschul, S.F., Madden, T.L., Schäffer, A.A., Zhang, J., Zhang, Z., Miller, W., Lipman, D.J., 1997. Gapped BLAST and PSI–BLAST: a new generation of protein databases search programs. Nucleic Acids Res. 25, 3389–3402.

Balboa, S., 2012. Study of the intraspecific variability of the clam pathogen *Vibrio tapetis*. Ph.D. thesis. University of Santiago de Compostela, Spain.

Beaz−Hidalgo, R., Balboa, S., Romalde, J.L., Figueras, M.J., 2010. Diversity and pathogenecity of *Vibrio* species in cultured bivalve molluscs. Environ. Microbiol. Rep. 2, 34–43.

Binesse, J., Delsert, C., Saulnier, D., Champomier–Vergés, M.C., Zagorec, M., Munier–Lehmann, H., Mazel, D., Le Roux, F., 2008. Metalloprotease Vsm is the major determinant of toxicity for extracellular products of *Vibrio splendidus*. Appl. Environ. Microbiol. 74, 7108–7117.

Boardman, B.K., Meehan, B.M., Satchell, K.J.F., 2007. Growth phase regulation of *Vibrio cholerae* RTX toxin export. J. Bacteriol. 189, 1827–1835.

Cabello, A.E., Espejo, R.T., Romero, J., 2005. Tracing *Vibrio parahaemolyticus* in oysters (*Tiostrea chilensis*) using a green fluorescent protein tag. J. Exp. Mar. Bio. Ecol. 327, 157–166.

Cardinaud, M., Barbou, A., Capitaine, C., Bidault, A., Dujon, A.M., Moraga, D., Paillard, C., 2014. *Vibrio harveyi* adheres to and penetrates tissues of the european

abalone *Haliotis tuberculata* within the first hours of contact. Appl. Environ. Microbiol. 80, 6328–6333.

Chaand, M., Miller, K.A., Sofia, M.K., Schlesener, C., Weaver, J.W.A., Sood, V., Dziejman, M., 2015. Type three secretion system island–encoded proteins required for colonization by non–O1/non–O139 serogroup *Vibrio cholerae*. Infect. Immun. 83, 2862–2869.

Cheng, Q., Li, H., Merdek, K., Park, J.T., 2000. Molecular characterization of the beta–N–acetylglucosaminidase of *Escherichia coli* and its role in cell wall recycling. J. Bacteriol. 182, 4836–4840.

Chudakov, D.M., Matz, M.V., Lukyanov, S., Lukyanov, K., 2010. Fluorescent proteins and their applications in imaging living cells and tissues. Physiol. Rev. 90, 1103–1163.

DeLoney–Marino, C.R., Wolfe, A.J., Visick, K.L., 2003. Chemoattraction of *Vibrio fischeri* to serine, nucleosides, and N–acetylneuraminic acid, a component of squid light–organ mucus. Appl. Environ. Microbiol. 69, 7527–7530.

Dubert, J., Romalde, J.L., Prado, S., Barja, J.L., in press. *Vibrio bivalvicida* sp. nov., a novel larval pathogen for bivalve molluscs reared in hatchery. Syst. Appl. Microbiol.

Elston, R., 1980a. Functional anatomy, histology and ultrastructure of the soft tissues of the larval american oyster *Crassostrea virginica*. Proc. Nat. Shellfish. Assoc. 70, 65–93.

Elston, R., 1980b. Functional morphology of the coelomocytes of the larval oysters (*Crassostrea virginica* and *Crassostrea gigas*). J. Mar. Biol. Assoc. U.K. 60, 947–957.

520 Elston, R., Leibovitz, L., 1980. Pathogenesis of experimental vibriosis in larval
521 American oysters, *Crassostrea virginica*. Can. J. Fish Aquat. Sci. 37, 964–978.
522 Gómez–León J., Villamil, L., Lemos, M.L., Novoa, B., Figueras, A., 2005. Isolation of
523 *Vibrio alginolyticus* and *Vibrio splendidus* from aquacultured carpet shell clam
524 (*Ruditapes decussatus*) larvae associated with mass mortalities. Appl. Environ.
525 Microbiol. 71, 98–104.
526 Gómez–León, J., Villamil, L., Salger, S.A., Sallum, R.H., Remacha–Triviño, A.,
527 Leavitt, D.F., Gómez–Chiarri, M., 2008. Survival of eastern oysters *Crassostrea*
528 *virginica* from three lines following experimental challenge with bacterial
529 pathogens. Dis. Aquat. Org. 79, 95–105.
530 Grisez, L., Chair, M., Sorgeloos, P., Ollevier, F., 1996. Mode of infection and spread of
531 *Vibrio anguillarum* in turbot *Scophthalmus maximus* larvae after oral challenge
532 through live feed. Dis. Aquat. Org. 26, 181–187.
533 Hasegawa, H., Lind, E.J., Boin, M.A., Häse, C.C., 2008. The extracellular
534 metalloprotease of *Vibrio tubiashii* is a major virulence factor for pacific oyster
535 (*Crassostrea gigas*) larvae. Appl. Environ. Microbiol. 74, 4101–4110.
536 Johnson, T.L., Fong, J.C.N., Rule, C., Yildiz, F.H., Sandkvist, M., 2014. The Type II
537 secretion system delivers matrix proteins for biofilm formation by *Vibrio*
538 *cholerae*. J. Bacteriol. 196, 4245–4252.
539 Kasyanov, V.L., Kryuchkova, G.A., Kulikova, V.A., Medvedeva, L.A., 1998. Larvae of
540 marine bivalves (morphology, physiology and behavior). In: Pawson, D.L. (Ed.),
541 Larvae of marine bivalves and echinoderms, Smithsonian Institution Libraries,
542 Washington DC, pp. 1–104.

543 Korotkov, K.V., Sandkvist, M., Hol, W.G.J., 2012. The type II secretion system:
544 biogenesis, molecular architecture and mechanism. Nat. Rev. Microbiol. 10, 336–
545 351.
546 Kudryashev, M., Wang, R.Y.R., Brackmann, M., Scherer, S., Maier, T., Baker, D.,
547 DiMaio, F., Stahlberg, H., Egelman, E.H., Basler, M., 2015. Structure of the type
548 VI secretion system contractile sheath. Cell 160, 952–962.
549 Labreuche, Y., Le Roux, F., Henry, J., Zatylny, C., Huvet, A., Lambert, C., Soudant, P.,
550 Mazel, D., Nicolas, J.L., 2010. *Vibrio aestuarianus* zinc metalloprotease causes
551 lethality in the pacific oyster *Crassostrea gigas* and impairs the host cellular
552 immune defense. Fish Shellfish Immunol. 29, 753–758.
553 Lane, D.J., 1991.16S/23S rRNA sequencing. In: Stackebrandt, E., Goodfellow, M.
554 (Eds.), Nucleic acid techniques in bacterial systematics, John Wiley & Sons, New
555 York, pp. 115–175.
556 Larsen, M.H., Blackburn, N., Larsen, J.L., Olsen, J.E., 2004. Influences of temperature,
557 salinity and starvation on the motility and chemotactic response of *Vibrio*
558 *anguillarum*. Microbiology 150, 1283–1290.
559 Lindell, K., Fahlgren, A., Hjerde, E., Willassen, N.P., Fällman, M., Milton, D.L., 2012.
560 Lipopolysaccharide O–antigen prevents phagocytosis of *Vibrio anguillarum* by
561 rainbow trout (*Oncorhynchus mykiss*) skin epithelial cells. PLoS ONE 7(5),
562 e37678.
563 Lu, X., Liang, W., Wang, Y., Xu, J., Zhu, J., Kan, B., 2014. Identification of genetic
564 bases of *Vibrio fluvialis* species–specific biochemical pathways and potential
565 virulence factors by comparative genomic analysis. Appl. Environ. Microbiol. 80,
566 2029–2037.

Magariños, B., Santos, Y., Romalde, J.L., Rivas, C., Barja, J.L., Toranzo, A.E., 1992. Pathogenic activities of live cells and extracelular products of the fish pathogen *Pasteurella piscicida.* J. Gen. Microbiol. 138, 2491–2498.

Majumdar, A., Ghatak, A., Ghosh, R.K., 2005. Identification of the gene for the monomeric alkaline phosphatase of *Vibrio cholerae* serogroup O1 strain. Gene 344, 251–248.

Mersni–Achour, R., Imbert–Auvray, N., Huet, V., Cheikh, J.B., Faury, N., Doghri, I., Rouatbi, S., Bordenave, S., Travers, M.A., Saulnier, D., Fruitier–Arnaudin, I., 2014. First description of French *V. tubiashii* strains pathogenic to mollusk: II. Characterization of properties of the proteolytic fraction of extracellular products. J. Invertebr. Pathol. 123, 49–59.

Milton, D.L., Norqvist, A., Wolf–Watz, H., 1992. Cloning of a metalloprotease gene involved in the virulence mechanism of *Vibrio anguillarum*. J. Bacteriol. 174, 7235–7244.

Norqvist, A., Norrman, B., Wolf–Watz, H., 1990. Identification and characterization of a zinc metalloprotease associated with invasion by the fish pathogen *Vibrio anguillarum*. Infec. Immun. 58, 3731–3736.

O'Toole, R., Lundberg, S., Fredriksson, S.Å., Jansson, A., Nilsson, B., Wolf–Watz, H., 1999. The chemotactic response of *Vibrio anguillarum* to fish intestinal mucus is mediated by a combination of multiple mucus components. J. Bacteriol. 181, 4308–4317.

Olsson, J.C., Jöborn, A., Westerdahl, A., Blomberg, L., Kjelleberg, S., Conway, P.L., 1996. Is the turbot, *Scophthalmus maximus* (L.), intestine a portal of entry for the fish pathogen *Vibrio anguillarum*?. J. Fish. Dis. 19, 225–234.

591 Piekarski, T., Buchholz, I., Drepper, T., Schobert, M., Wagner–Doebler, I., Tielen, P.,
592 Jahn D., 2009. Genetic tools for the investigation of *Roseobacter* clade bacteria.
593 BMC Microbiol. 9:265.
594 Prado, S., Dubert, J., Barja, J.L., 2015. Characterization of pathogenic Vibrio spp.
595 isolated from bivalve hatcheries in Galicia, NW Atlantic coast of Spain.
596 Description of *Vibrio tubiashii* subsp. *europaensis* subsp. nov. Syst. Appl.
597 Microbiol. 38, 26−29.
598 Prado, S., Romalde, J.L., Montes, J., Barja, J.L., 2005. Pathogenic bacteria isolated
599 from disease outbreaks in shellfish hatcheries. First description of *Vibrio*
600 *neptunius* as an oyster pathogen. Dis. Aquat. Org. 67, 209−215.
601 Rekecki, A., Gunasekara, R., Dierckens, K., Laureau, S., Boon, N., Favoreel, H.,
602 Cornelissen, M., Sorgeloos, P., Ducatelle, R., Bossier, P., Van den Broeck, W.,
603 2012. Bacterial host interaction of GFP–labelled *Vibrio anguillarum* HI–610 with
604 gnotobiotic sea bass, *Dicentrarchus labrax* (L.), larvae. J. Fish Dis. 35, 265–273.
605 Rojas, R., Miranda, C.D., Opazo, R., Romero, J., 2015. Characterization and
606 pathogenicity of *Vibrio splendidus* strains associated with massive mortalities of
607 commercial hatchery–reared larvae of scallop *Argopecten purpuratus* (Lamarck,
608 1819). J. Invertebr. Pathol. 124, 61–69.
609 Romalde, J.L., 1992. *Yersinia ruckeri*: Estudio epidemiológico y del mecanismo de
610 virulencia. Ph.D. thesis. University of Santiago de Compostela, Spain.
611 Sheng, L., Lv, Y., Liu, Q., Wang, Q., Zhang, Y., 2013. Connecting type VI secretion,
612 quorum sensing, and c–di–GMP production in fish pathogen *Vibrio alginolyticus*
613 through phosphatase PppA. Vet. Microbiol. 162, 652–662.
614 Shinoda, S., Miyoshi, S.I., 2011. Proteases produced by Vibrio spp.. Biocontrol Sci. 16,
615 1−11.

Sikora, A.E., 2013. Proteins secreted via the Type II secretion system: smart strategies of *Vibrio cholerae* to maintain fitness in different ecological niches. PLoS Pathog. 9(2), doi:10.1371/journal.ppat.1003126.

Suginta, W., Chuenark, D., Mizuhara, M., Fukamizo, T., 2010. Novel β–N–acetylglucosaminidases from *Vibrio harveyi* 650: cloning, expression, enzymatic properties, and subsite identification. BMC Biochem. 11:40.

Torrecillas, S., Makol, A., Benítez–Santana, T., Caballero, M. J., Montero, D., Sweetman, J., Izquierdo, M., 2011. Reduced gut bacterial translocation in European sea bass (Dicentrarchus labrax) fed mannan oligosaccharides (MOS). Fish Shellfish Immunol. 3, 674–681.

Travers, M.A., Barbou, A., Le Goïc, N., Huchette, S., Paillard, C., Koken, M., 2008. Construction of a stable GFP–tagged *Vibrio harveyi* strain for bacterial dynamics analysis of abalone infection. FEMS Microbiol. Lett. 289, 34–40.

Travers, M.A., Mersni–Achour, R., Haffner, P., Tourbiez, D., Cassone, A.L., Morga, B., Doghri, I., Garcia, C., Renault, T., Fruitier–Arnaudin, I., Saulnier, D., 2014. First description of French *V. tubiashii* strains pathogenic to mollusk: I. Characterization of isolates and detection during mortality events. J. Invertebr. Pathol. 123, 38–48.

Tubiash, H.S., Chanley, P.E., Leifson, E., 1965. Bacillary necrosis, a disease of larval and juvenile bivalve mollusks I. Etiology and epizootiology. J. Bacteriol. 90, 1036–1044.

Varina, M., Denkin, S.M., Staroscik, A.M., Nelson, D.R., 2008. Identification and characterization of Epp, the secreted processing protease for the *Vibrio anguillarum* EmpA metalloprotease. J. Bacteriol. 190, 6589–6597.

640 Zhang, L., Krachler, A.M., Broberg, C.A., Li, Y., Mirzaei, H., Gilpin, C.J., Orth, K.,
641 2012. Type III effector VopC mediates invasion for *Vibrio* species. Cell Rep 1,
642 453–460.
643 Zhao, W., Dao, C., Karim, M., Gomez–Chiarri, M., Rowley, D., Nelson, D.R.,
644 unpublished results. Contributions of tropodithietic acid and biofilm formation to
645 the probiotic activity of *Phaeobacter gallaeciensis*. BMC Microbiol.
646

Figure legends

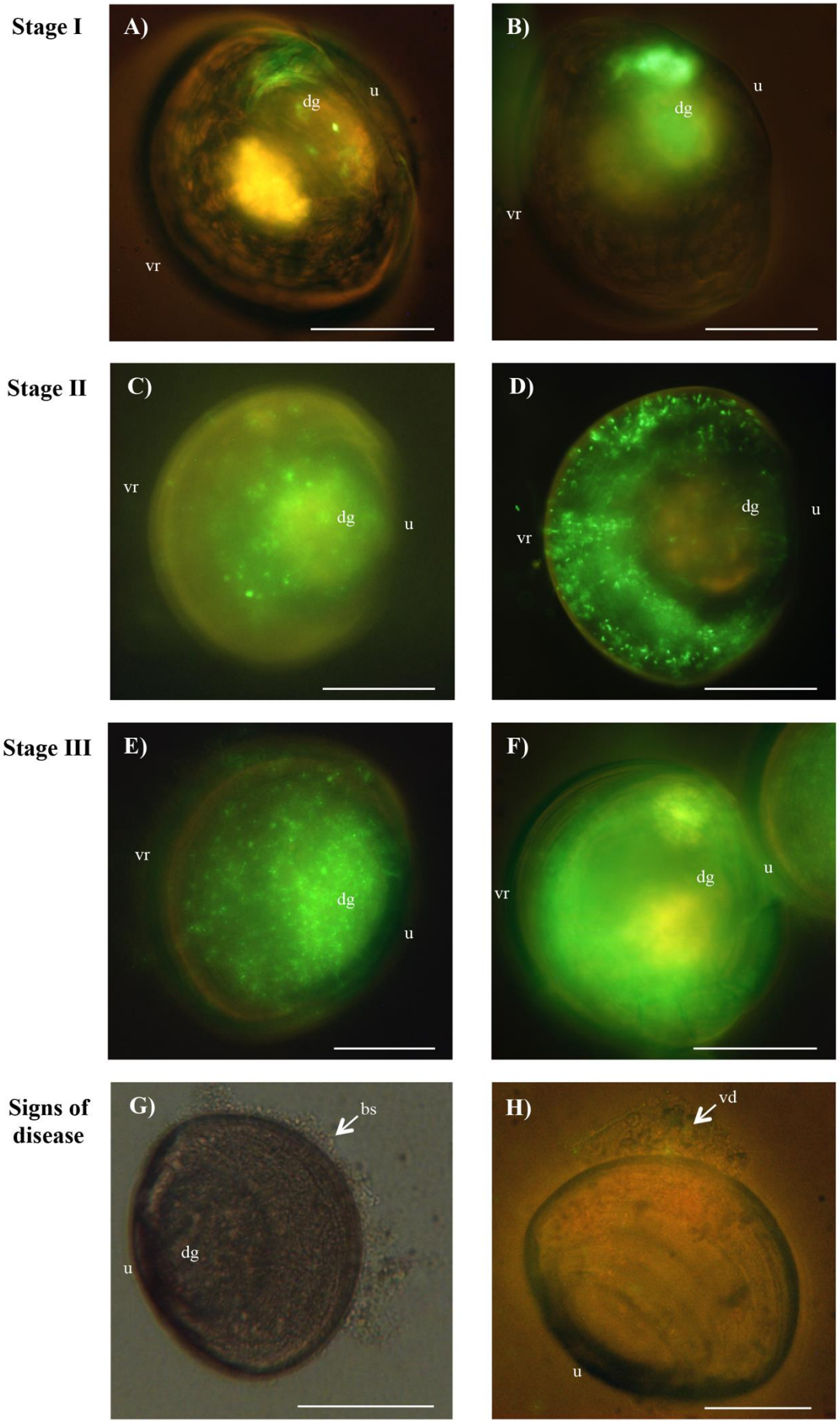
Stage I
A)
dg
u
vr
B)
u
dg
vr
Stage II
C)
vr
dg
u
D)
dg
u
vr
Stage III
E)
vr
dg
u
F)
dg
u
vr
Signs of disease
G)
bs
dg
u
H)
vd
u

648

Fig. 1. Progression of the infection by pathogenic *Vibrio* spp. in Manila clam larvae determined by epifluorescence microscope (40x): Stage I at 2 h (A–B); Stage II at 6 h (C) and 8 h (D); Stage III at 14 h (E) and 24 h (F); dg: digestive gland; i, intestine; u: umbo; vr: ventral region. Autofluorescence in the retracted vellum (v) in A and B was due to autofluorescence of microalgae under epifluorescence microscopy. Signs of disease after 24 h, ubiquitous bacterial swarming (bs) around the dead larvae (G) observed by phase contrast in inverted microscope (20x); Velum disruption (vd) after all other soft tissues have been destroyed (H) determined by epifluorescence microscope (40x). Scale bars: 50 μm.